

Small angle x-ray scattering metrology for sidewall angle and cross section of nanometer scale line gratings

Tengjiao Hu, Ronald L. Jones, Wen-li Wu,^{a)} and Eric K. Lin
*Polymers Division, MSEL, National Institute of Standards and Technology, Gaithersburg,
Maryland 20899-8541*

Qinghuang Lin
IBM Thomas J. Watson Research Center, P.O. Box 218, Yorktown Heights, New York 10598

Denis Keane, Steve Weigand, and John Quintana
DND-CAT, Advanced Photon Source, Argonne National Laboratory, Argonne, Illinois 60439

(Received 15 March 2004; accepted 25 May 2004)

High-volume fabrication of nanostructures requires nondestructive metrologies capable of measuring not only the pattern size but also the pattern shape profile. Measurement tool requirements will become more stringent as the feature size approaches 50 nm and tolerances of pattern shape will reach a few nanometers. A small angle x-ray scattering (SAXS) based technique has been demonstrated to have the capability of characterizing the average pitch size and pattern width to subnanometer precision. In this study, we report a simple, modeling-free protocol to extract cross-section information such as the average sidewall angle and the pattern height of line grating patterns from the SAXS data. Diffraction peak intensities and reciprocal space positions are measured while the sample is rotated around the axis perpendicular to the grating direction. Linear extrapolations of peak positions in reciprocal space allow a precise determination of both the sidewall angle and the pattern height. © 2004 American Institute of Physics.

[DOI: 10.1063/1.1773376]

INTRODUCTION

Nanometer scale control of lithographic pattern quality is required as the semiconductor industry moves to mass production of sub-100 nm devices.¹ Specifically, metrologies capable of providing information on the cross section of patterns are a critical component to the development of practical high-volume nanofabrication methods. Scanning electron microscopy (SEM) has been the mainstay inspection metrology in lithography.^{2,3} Other methods, such as atomic force microscopy (AFM) and light scatterometry,⁴⁻⁶ have been proposed as alternative methods to measure pattern quality. All of these techniques face challenges as device features continue to shrink to the scale of tens of nanometers. For example, these three metrologies are expected to face challenge in measuring dense, high aspect ratio, as well as buried features, with decreasing feature size.⁷⁻⁹ As a result, the development of a metrology for measuring a sidewall angle close to zero degrees and line-edge roughness (LER) on the scale of only a few nanometers is listed as one of the five major inspection metrology challenges in the most recent "International Technology Roadmap for Semiconductors" (ITRS).¹⁰

A technique based on small angle x-ray scattering (SAXS) has been introduced as an alternative to current measurement methods to characterize patterns with a critical dimension (CD) on the scale of nanometers.¹¹⁻¹³ Critical dimension-small angle x-ray scattering (CD-SAXS) has sev-

eral potential advantages over existing inspection metrologies including increased sensitivity to smaller features and a capability of measuring dense high aspect ratio patterns or buried patterns. Earlier results have demonstrated that CD-SAXS can provide a fast and accurate measurement of the average pitch size and pattern width of testing grating patterns from the position and relative scattering intensity of diffraction peaks. However, elements of the measured data suggest that more detail about pattern shape and quality can be extracted with more refined methods of analysis. As an example, the peak intensity along the diffraction axis decays more rapidly than predicted from a simple rectangular model for the pattern profile.¹³ A more rapid decay has many potential origins such as a random deviation in pitch size, line-edge roughness (LER), and a nonrectangular grating shape profile. This information is critical for the manufacture of nanometer scale devices.¹⁴

In this paper, we describe a general methodology for measuring the cross section of grating patterns. We then apply the methodology to extract the average sidewall angle of photoresist gratings prepared by optical lithography. In this particular case, a trapezoid is used to model the cross section. Thus, analysis of SAXS data can provide the entire cross section of the pattern as well as the average pitch size and pattern width. The results are compared to cross-sectional SEM images of the same patterns.

EXPERIMENT

The samples consist of a series of equally spaced parallel lines prepared directly on a 200 mm diam single crystal sili-

^{a)}Author to whom correspondence should be addressed; electronic mail: wen-li.wu@nist.gov

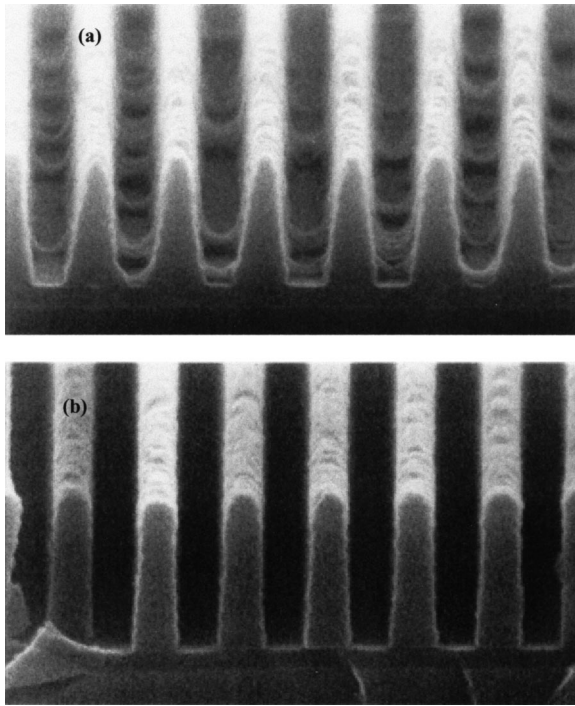


FIG. 1. SEM micrograph of the grating patterns with $+0.4$ and $+0.2$ μm of focus depth deviation from optimal imaging conditions.

con wafer. 248 nm optical lithography was used to produce this grating structure with a nominal 150 nm linewidth and a 1:1 line space ratio. The samples discussed here are labeled as sample A and B, and were imaged with a depth of focus deviation from the optimal condition by 0.4 μm and 0.2 μm , respectively. Cross-sectional SEM images (Fig. 1) taken with a tilt angle of 30° indicate that the cross section (in X-Z plane defined in Fig. 2) of the patterns is approximately trapezoidal with a noticeable difference between the sidewall angles for these two samples. The sidewall angle from the SEM image of sample A is estimated to be 7° and its precise value is not available since the micrograph (Fig. 1) was not taken from a quantitative SEM.

For the purpose of demonstrating the principle synchrotron x-ray source has been used. However, in the previous paper¹² the feasibility of using a laboratory x-ray source for

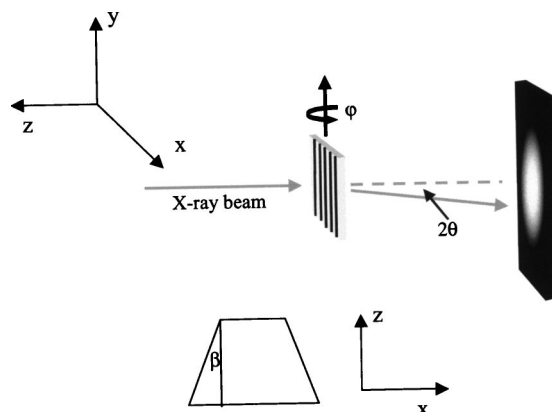


FIG. 2. Schematic of the small angle x-ray scattering geometry illustrating the scattering angle 2θ , the sample rotation angle φ , and sample sidewall angle β .

CD measurements was discussed. A molybdenum x-ray source with the state of art optics and detector is now under consideration for this purpose. The CD-SAXS measurements were performed at the 5ID-DND beamline of the Advanced Photon Source (Argonne National Laboratory) using a 2D CCD detector. The x-ray wavelength was set to (0.7289 ± 0.001) \AA using a double monochromator.¹⁵ At this wavelength, there is still a transmission of approximately 20% of the incident beam through standard silicon wafers. The beam was collimated by two sets of slits to a size of (120×180) μm^2 as measured at the sample position. In these experiments, a smaller beam size is not necessary. However, a further decrease of beam size to characterize standard industrial test structures, over an area of about (50×50) μm^2 , is feasible as demonstrated in our earlier experiments. One ion chamber was used to monitor the incident beam intensity. No large intensity fluctuations or drift of the incident beam was observed during the measurement. The sample was rotated around the Y axis, as defined in Fig. 2, from nominal -20° to 20° with a step size of $(1 \pm 0.05)^\circ$. The 2D detector was placed (700 ± 1) cm from the sample. The detector has a resolution of (78.75 ± 0.01) μm per pixel with 2048 pixels in each direction. In contrast to our prior experiments, the air scattering is greatly reduced here with the use of an evacuated sample chamber with a pressure on the order of 10^{-1} Pa.

In order to make a consistent comparison between scattering data from different rotation angles, a correction of the beam path length is necessary due to the attenuation of the x-ray beam by the silicon substrate. As we rotate the sample, the effective transmission path changes as $d/\cos \varphi$, where d is the thickness of the silicon substrate (approximately 1 mm). The pattern height (approximately 0.3 μm) is negligible in this correction.

RESULTS AND DISCUSSION

The average cross section of the grating patterns is modeled as a trapezoid. The predicted scattering intensity contours in Fourier space representing the form factor of an isolated trapezoid are shown in Fig. 3. For clarity a 3D representation of the form factor is also provided in this figure. In this plot, the bevel edges of the patterns result in a series of scattering peaks along lines offset at an angle of $\pm\beta$ from the q_x axis in the q_x - q_z plane. The constructive interference of scattered x-ray from multiple periodically arranged trapezoids results in vertical ridges with a spacing of $2\pi/D$, where D is the pitch of the grating. The complete Fourier transform of the grating structure is therefore described as a set of vertical ridges with positions defined by the reciprocal lattice of the grating and intensities defined by the form factor of an isolated trapezoid.

The determination of the pattern cross section requires a measurement of the scattered intensity in the q_x - q_z plane. However, in earlier work, the beam was normal to the substrate and primarily probed the scattering in q_x - q_y plane, with a limited range in q_z at larger scattering angles. There are several approaches to probe the q_z dependence of the scattering intensity. One is to measure the scattering at a very

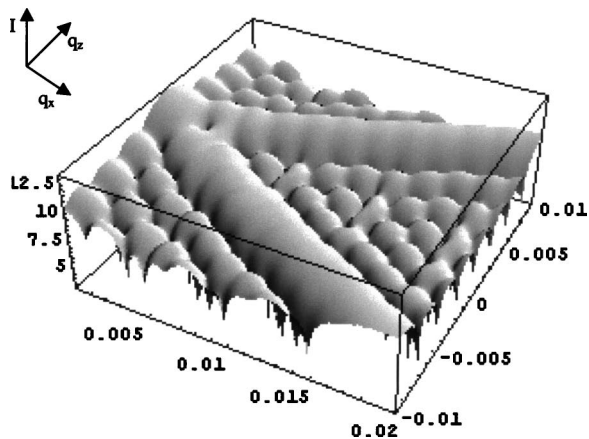
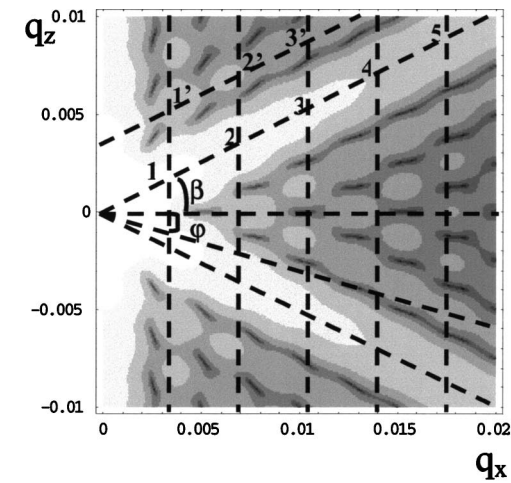


FIG. 3. Contour plot of the scattering intensity based on the analytical form factor for a trapezoidal cross section on the q_x - q_z plane. The lattice points of an equally spaced grating are given as a set of vertical lines. The Ewald sphere is approximately depicted as a straight line at a rotation angle φ . The dimensions of the trapezoid used in this calculation are: height=2000 Å, width at middle=1200 Å, sidewall angle $\beta=26.57^\circ$, repeat of the grating=2000 Å. A 3D presentation of the above contour plot of the form factor alone is also given.

large scattering angle, where the q_z dependence of the scattering intensity cannot be neglected. Another approach is to vary the x-ray wavelength, which will push the surface of the Ewald sphere forward or backward (i.e., probing different q_z 's). But, the diffraction peak intensity decays very fast as the scattering angle increases. In addition, a variation of the x-ray wavelength is not always convenient or practical. A third method of probing q_z dependence is to measure the small angle scattering from samples at different sample rotation angles, φ , as indicated in Fig. 2. Experimentally, diffraction peaks occur at the intersections between the reciprocal lattice and the Ewald sphere in the q_x - q_y plane. By collecting data over a range of φ , the reciprocal space map of the sample is rotated relative to the Ewald sphere, and the positions of the diffraction peaks can be transformed back to the original q_x - q_z plane. In this way, the theoretical map of Fig. 3 can be obtained. The advantage of this approach is the use of the small q_x regime, providing relatively high signal to noise data over the alternative methods.

Using the sample rotation protocol, the intensity of a given diffraction peak as a function of sample rotation angle,

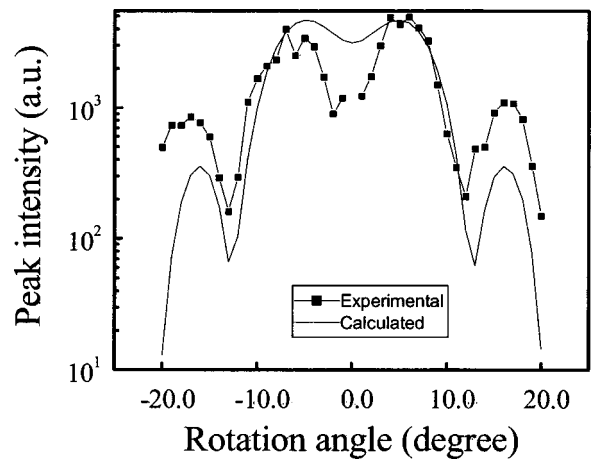


FIG. 4. Experimental data of sample A and the corresponding theoretically calculated peak intensities of the fifth order diffraction at different rotation angles.

φ , traces a vertical line in Fig. 3 (i.e., approximately constant q_x). The direct correspondence of the angle between the line traced by the peak positions in Fig. 3 and the sidewall angle, β , provides a simple and intuitive way to extract the average sidewall angle from scattering data. It further suggests that the scattering intensity of all diffraction orders reaches a maximum as the rotation angle φ approaches β .

Figure 4 shows the rotation angle dependence of the peak intensity for the fifth order diffraction peak. The midpoint between the two primary peaks was chosen as the origin (i.e., $\varphi=0$) on the abscissa because of a lack of precise sample alignment in the current experimental system. However, this step is not necessary if high precision sample alignment equipment is utilized for future work. The theoretically calculated peak intensity with only one varying parameter (the sidewall angle of the pattern) shows a qualitative agreement with the experimental data. The fitting result gives a sidewall angle of $\approx 5^\circ$. Good agreement between the experimental values and the calculated ones was also observed for the second maximum in Fig. 4. In contrast to the complicated modeling required to build data libraries in light scatterometry, CD-SAXS provides an estimate of the average sidewall angle of the sample simply by locating the sample rotation angle φ where every diffraction peak reaches its global maximum. No data modeling or fitting is required for this procedure. The results from sample B indicate that the sidewall angle is $\approx 3.0^\circ$. These results agree qualitatively with the SEM results given in Fig. 1.

Also in Fig. 4, the observed peak intensity shows multiple maxima and minima as a function of the rotation angle. Figure 5 provides a set of calculated results of the peak intensity of the fifth, sixth, and seventh order diffraction peaks over a range of φ for a sidewall angle of 5° . Regardless of the peak order, all intensities reach their global maximum at the same rotation angle φ . However, the rotation angle spacing between maxima for higher order peaks is smaller than lower order peaks. This can be understood from Fig. 3 where the line representing the Ewald sphere touches point 3' at lower φ than that for point 1'.

While the approach demonstrated in Fig. 4 can provide

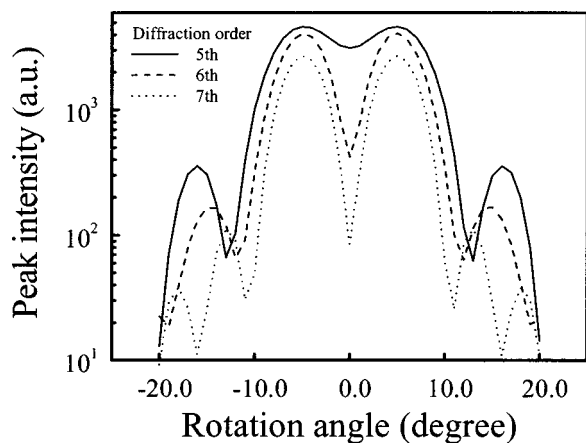


FIG. 5. Calculated rotation angle dependence of the diffraction peak intensities at three different diffraction orders. The sidewall angle in the model is 5.0°.

an estimate of the sidewall angle, one can enhance the precision by analyzing the entire data set collectively. To illustrate this higher precision approach, data from Sample A are used to determine the sidewall angle. In Fig. 6, we plot the positions of the maxima and minima of all the observed peaks in terms of their coordinates on the q_x - q_z plane. The positions of the diffraction peaks follow the form predicted theoretically in Fig. 3. Importantly, linear extrapolations through the positions of the first maxima from both positive and negative q_z branches intersect the origin of the q_x - q_z plane providing confidence in the q_x - q_z values. However, in this representation of the data, the lines within each positive and negative branch of q_z are not perfectly parallel. This is especially obvious for the first minima data points. This deviation may have several origins. One possibility is that the cross section of the pattern is not a trapezoid. However, the linearity of the q_z with respect to q_x in Fig. 6 shows that the trapezoid model is at the least a good approximation of the average cross section in our case. In addition, uncertainties in the determination of q_x and q_z may arise from imperfect sample alignment with respect to the incident beam or small rotational offset differences between the rotation axis and

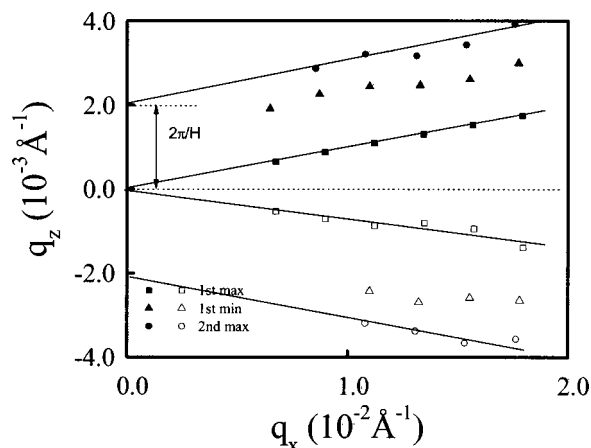


FIG. 6. Diffraction peak positions of the maxima and minima intensities of sample A in the q_x - q_z plane. Lines are drawn to connect the observed maxima.

Y -axis. These shortfalls can be overcome with a high precision sample alignment tool. Finally, the intensity around the minima is not distinguishably higher than the background scattering. This causes a significant uncertainty in determining the actual position of the minima. Therefore, only peak maxima data points were used for sidewall angle determination. Using the linear fits of the major maxima, we determine an effective sidewall angle of $(5.7 \pm 0.2)^\circ$ for sample A.

In this analysis, we plot and analyze only the positions of the maxima and minima. We clearly demonstrate a capacity for accurate determination of the average cross section of patterns. In future efforts, more detailed information on the cross-sectional shape such as higher order deviations from a simple trapezoid can be deduced through more detailed, but straightforward modeling efforts that account not only for the peak positions on the q_x - q_z plane, but also all the observed peak intensities. For patterns with ever shrinking feature size, this approach can be readily applied with x-ray equipment of less stringent resolution requirements, e.g., quantitative lattice information on protein crystals has routinely been deduced using today's laboratory based x-ray equipment. Patterns with feature size of a few nanometers such as protein crystals are accurately easier to characterize using x ray than patterns with 100 nm periodicity.

In our previous publication, we proposed to obtain the pattern height from the absolute intensity of diffraction peaks provided that the scattering cross section of the grating material is given. Since experimental data are now available over a wide q_z range as given in Fig. 6, we can determine the pattern height from the intercept of a line connecting the secondary maxima (i.e., 1', 2', 3', etc. in Fig. 3). The height, H , of the trapezoid is simply related to the intercept via $2\pi/\Delta q_z$, where Δq_z is the value of the intercept of the line, as given in Fig. 6. For sample A, the height is ≈ 318 nm, which is consistent with the result from fitting the relative peak intensity data. This provides a preferable way to obtain pattern height since there is no need for a prior knowledge of the scattering cross section of the grating materials and the scattering intensity observed does not need to be reduced to its absolute scale.

SUMMARY

Inspection of the cross-sectional profile for lithographic patterns has been listed as one of the five major challenges in the recent revised version of ITRS. Building upon the recently proposed CD-SAXS metrology, we further developed a protocol to determine sidewall angle of patterns by collecting scattering data at various rotation angles. For illustration, a simple trapezoidal cross section was chosen to model the sample scattering. Data from two line grating samples were collected and analyzed in terms of the positions of the intensity maxima and minima of the diffraction peaks as the sample is rotated. The sidewall angle determined is qualitatively in agreement with those observed in SEM micrographs. In addition, this method also provides a convenient measurement of pattern height. Work is in progress to deduce

sidewall roughness from the scattering data, primarily from the scattering intensities along the q_y direction at each node.¹⁶

ACKNOWLEDGMENTS

This work was funded in part by the DARPA Advanced Lithography Program under Contract No. N66001-00-C-8083. Additional funding was provided by the NIST Office of Microelectronics Programs. R. L. J. is supported by a National Research Council-NIST postdoctoral fellowship.

¹H. M. Marchman, J. E. Griffith, J. Z. Y. Guo, J. Frackowiak, and G. K. Celler, *J. Vac. Sci. Technol. B* **12**, 3585 (1994).

²Li-Jui Chen, Shang-Wei Lin, Tsai-Sheng Gau, and Burn J. Lin, *Proc. SPIE* **5038**, 166 (2003).

³Eric Solecky, Chas Archie, Jason Mayer, Roger Cornell, and Ofer Adan, *Proc. SPIE* **5038**, 518 (2003).

⁴Ronald Dixson, Angela Guerry, Marylyn Bennett, Theodore Vorburger, and Ben Bunday, *Proc. SPIE* **5038**, 150 (2003).

⁵Eytan Barouch and Stephen L. Knodle, *Proc. SPIE* **5038**, 559 (2003).

⁶Li-Jui Chen, Chih-Ming Ke, Shinn-Sheng Yu, Tsai-Sheng Gau, Pei-Hung

Chen, Yao-Ching Ku, and Burn J. Lin, *Proc. SPIE* **5038**, 568 (2003).

⁷A. V. Nikitin, A. Sicignano, D. Y. Yerebin, M. Sandy, and T. Goldburt, *Proc. SPIE* **5038**, 651 (2003).

⁸Kouji Kimura, Kazuo Abe, Yasuko Tsuruga, Hitoshi, Nobuo Kochi, Hitotami Koike, and Yuichiro Yamazaki, *Proc. SPIE* **5038**, 1089 (2003).

⁹B. C. Park, J. Kang, K. Y. Jung, W. Y. Song, B.-h. O, and T. B. Eom, *Proc. SPIE* **5038**, 935 (2003).

¹⁰*International Technology Roadmap for Semiconductors*, <http://public.itrs.net/Files/2003ITRS/Home2003.htm>, 2003.

¹¹Wen-li Wu, Eric K. Lin, Qinghuang Lin, and Marie Angelopolous, *J. Appl. Phys.* **88**, 7298 (2000).

¹²Ronald L. Jones, Tengjiao Hu, Eric K. Lin, Wen-li Wu, Rainer Kolb, Diego M. Casa, Patrick J. Bolton, and George G. Barclay, *Appl. Phys. Lett.* **83**, 4059 (2003).

¹³Tengjiao Hu, Ronald L. Jones, Wen-li Wu, Christopher Soles, Eric K. Lin, Arpan Mahorowala, and Diego M. Casa, *Polym. Prepr. (Am. Chem. Soc. Div. Polym. Chem.)* **44**, 541 (2003).

¹⁴A. Guinier, *X-Ray Diffraction in Crystals, Imperfect Crystals, and Amorphous Bodies* (Dover, New York, 1994).

¹⁵The data in this manuscript and in the figures are presented along with the standard uncertainty (\pm) involved in the measurement, where the uncertainty represents one standard deviation from the mean.

¹⁶Ronald L. Jones, Tengjiao Hu, Christopher L. Soles, Eric K. Lin, Wen-li Wu, Diego M. Casa, and Arpan Mahorowala, *Proc. SPIE* (in press).